

# Oligodendrocyte differentiation from adult multipotent stem cells is modulated by glutamate

F Cavaliere<sup>1</sup>, O Urria<sup>1</sup>, E Alberdi<sup>1</sup> and C Matute<sup>\*1</sup>

**We used multipotent stem cells (MSCs) derived from the young rat subventricular zone (SVZ) to study the effects of glutamate in oligodendrocyte maturation. Glutamate stimulated oligodendrocyte differentiation from SVZ-derived MSCs through the activation of specific *N*-methyl-D-aspartate (NMDA) receptor subunits. The effect of glutamate and NMDA on oligodendrocyte differentiation was evident in both the number of newly generated oligodendrocytes and their morphology. In addition, the levels of NMDAR1 and NMDAR2A protein increased during differentiation, whereas NMDAR2B and NMDAR3 protein levels decreased, suggesting differential expression of NMDA receptor subunits during maturation. Microfluorimetry showed that the activation of NMDA receptors during oligodendrocyte differentiation elevated cytosolic calcium levels and promoted myelination in cocultures with neurons. Moreover, we observed that stimulation of MSCs by NMDA receptors induced the generation of reactive oxygen species (ROS), which were negatively modulated by the NADPH inhibitor apocynin, and that the levels of ROS correlated with the degree of differentiation. Taken together, these findings suggest that ROS generated by NADPH oxidase by the activation of NMDA receptors promotes the maturation of oligodendrocytes and favors myelination.**

*Cell Death and Disease* (2012) 3, e268; doi:10.1038/cddis.2011.144; published online 2 February 2012

**Subject Category:** Neuroscience

Myelination and remyelination are critical steps for the correct functioning and repair of the central nervous system, as evidenced by the consequences of various demyelinating diseases. During early myelinogenesis, oligodendrocytes extend highly branched processes that contact and enwrap axons, forming the myelin sheath,<sup>1</sup> a process that results from oligodendrocyte-astrocyte-neuron cross talk. Thus, axonal signals control the timing of oligodendrocyte differentiation, as well as the activation of myelinogenesis.<sup>2</sup>

Understanding regarding the molecular signals that control multiple stages of oligodendrocyte and myelin development is needed in order to devise strategies for promoting myelin repair; pharmacological treatment for multiple sclerosis and other demyelinating diseases is still limited to palliative cures.<sup>3,4</sup> Myelin repair is critical to the outcome of demyelinating disorders because myelin/oligodendrocytes, in addition to axonal insulation, provide essential trophic support for long-term axonal survival (for a recent review, see Dutta and Trap<sup>5</sup>).

One possible strategy for remyelination is oligodendrocyte replacement. Adult oligodendrocytes are generated from oligodendrocyte precursor cells, which are derived from committed multipotent stem cells (MSCs; glial progenitors). Oligodendrogenesis is modulated by molecular pathways that commit neural stem cells and glial progenitors to the oligodendrocyte lineage. Adhesion molecules and cytoskeleton proteins have a critical role in the first step of this process; among which the expression of PSA-NCAM and nestin characterizes uncommitted neural progenitor cells.<sup>6,7</sup>

In addition, polydendrocytes, which also give rise to oligodendrocytes, express proteoglycan NG2.<sup>8</sup> Polydendrocytes are present in the subventricular zone (SVZ) and preferentially differentiate into oligodendrocytes, as well as, to a lesser extent, astrocytes and neurons.<sup>9</sup> Polydendrocytes express specific markers of oligodendrocyte differentiation, such as platelet-derived growth factor (PDGF) receptor  $\alpha$  and O4 that remain expressed until maturation, as well as Olig2, which is transiently modulated during differentiation. The persistence of polydendrocytes in the adult brain and the ability to generate oligodendrocytes suggests a potential use of these cells for cell replacement in demyelinating lesions.

Glutamate enhances the survival and proliferation of neural progenitors derived from the SVZ.<sup>10</sup> NG2 cells and oligodendrocytes express glutamate receptors,<sup>11</sup> which can trigger cell demise under pathological conditions.<sup>12,13</sup> In the present study, we aimed to analyze the effect of glutamate in modulating oligodendrocyte differentiation from a population of NG2-positive adult MSCs. We found that extracellular glutamate stimulates signaling at *N*-methyl-D-aspartate (NMDA) receptors, promoting oligodendrocyte differentiation and myelination from an adult multipotent stem cell population.

## Results

**Effect of glutamate on oligodendrocyte differentiation.** SVZ from young rats (P2–P4) were dissociated to obtain proliferating

<sup>1</sup>Department of Neurosciences and CIBERNED, University of Basque Country-UPV/EHU, E-48940 Leioa, Spain

\*Corresponding author: C Matute, Department of Neurosciences and CIBERNED, University of Basque Country-UPV/EHU, E-48940 Leioa, Spain.

Tel: +34 94 601 3244; Fax: +34 94 601 5055; E-mail: carlos.matute@ehu.es

**Keywords:** adult multipotent stem cells; oligodendrocyte differentiation; myelination; NADPH oxidase

**Abbreviations:** AMPA,  $\alpha$ -amino-3-hydroxy-5-methyl-4-isoxazolepropionic acid; DHPG, 3, 5-dihydroxyphenylglycine; EGF, epidermal growth factor; FGF, fibroblast growth factor; NMDA, *N*-methyl-D-aspartate; PEDF, pigment epithelium-derived factor; PDGF, platelet-derived growth factor; ROS, reactive oxygen species; SVZ, subventricular zone

Received 04.7.11; revised 13.12.11; accepted 14.12.11; Edited by A Verkhatzky

MSC. Cells were maintained for 7 days *in vitro* (DIV) in the presence of the mitogenic factors epidermal growth factor (EGF), bFGF and pigment epithelium-derived factor (PEDF) (Figure 1a). After 7 DIV, neurospheres were pre-committed to an oligodendrocytic phenotype for 3 days and differentiated for up to 10 days. Differentiation was calculated as the percentage of O4-positive cells among the total number of cells counterstained with Hoechst. We obtained 50% of differentiation after 1 day, 60% after 3 days and 72% after 7 days (Figure 1b). Decreasing number of O4-positive cells after 10 days was because of incoming cell death (data not shown). To investigate the effect of glutamate on oligodendrocyte differentiation, pre-committed neurospheres were differentiated for 3 days in the presence of glutamate receptor agonists (Figure 2a).

The proportion of O4-positive cells in oligodendrocyte differentiation medium (ODM) in the absence of glutamate was 53% (CTRL in Figure 2a). The addition of 1 mM glutamate to the medium increased the number of differentiated oligodendrocytes to 70%. This increase is visualized in Figure 2b with O4 immunostaining. However, lower concentrations of glutamate were ineffective. Similarly, activation of NMDA receptors with NMDA (100  $\mu$ M), in the presence of 100  $\mu$ M glycine, supported oligodendrocyte differentiation (Figure 2a). The pro-differentiating effects of both glutamate and NMDA were abolished by the NMDA receptor antagonist MK801 (Figure 2c). In contrast, selective activation of  $\alpha$ -amino-3-hydroxy-5-methyl-4-isoxazolepropionic acid (AMPA) and kainate receptors with AMPA and kainate in conjunction with GYKI53655 (100  $\mu$ M), respectively, did not affect differentiation rates (Figure 2a). The application of kainate alone (100  $\mu$ M) was toxic to the cells (data not shown, and

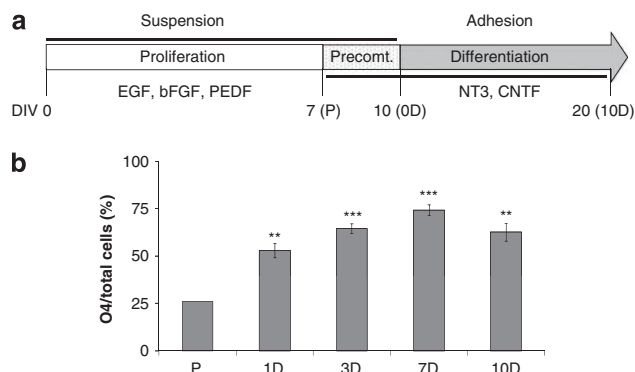


**Figure 1** Protocol used to obtain differentiated oligodendrocytes from SVZ-derived neurospheres. (a) Schematic view of the protocol showing the time course and culture conditions. During proliferation, cells were cultivated in suspension in the presence of 20 ng/ml EGF, 10 ng/ml bFGF, and 10 ng/ml PEDF. After 7 DIV, cells were pre-committed (Precomt.) to an oligodendrocyte phenotype in differentiation medium in the presence of 10  $\mu$ g/ml NT3 and 1  $\mu$ g/ml CNTF. Cultures were maintained for 3 days in suspension and then differentiated on cover slips treated with polyornithine in the same medium for up to 10 additional days. The beginning of differentiation was referred as 0D at the end of the pre-commitment period. (b) Histogram showing the proportion of differentiated oligodendrocytes identified by immunofluorescence with O4 antibody marker compared with the total number of cells revealed with Hoechst 33258 counterstaining. Counts were performed after 7 days of proliferation (P), and after different duration of differentiation (1, 3, 7, and 10 D). Counts represent means  $\pm$  S.E.M. ( $n=6$  independent experiments, five fields each). \*\* $P<0.01$ , \*\*\* $P<0.001$  compared with the proliferation stage

see Matute<sup>12</sup>). Finally, selective activation of mGluR1/5 with 50  $\mu$ M (S)-3,5-3, 5-dihydroxyphenylglycine (DHPG) decreased differentiation rate (13% with respect to control). This effect of DHPG was reverted by simultaneous application of DHPG with antagonist SIB 1757 (Figure 2c).

Glutamate-induced oligodendrocyte differentiation was further assessed by western blotting to determine CNPase protein levels. Glutamate induced a 44% increase in CNPase expression (Figure 2d), whereas the levels of NG2 protein decreased by 36% (Figure 2e). These findings indicate that glutamate increased the oligodendrocyte marker CNPase, which was accompanied by a reduction in the levels of the more immature marker NG2.

Glutamate and NMDA also affected oligodendrocyte morphology. Oligodendrocytes exposed to glutamate or NMDA had a more branched morphology, as illustrated by O4 staining (Figure 3). Quantification of the area covered by oligodendrocyte arborization indicated that glutamate and NMDA increased the area covered by the processes two- and threefold, respectively, an effect that was prevented by the NMDA receptor antagonist MK801. Taken together, these data indicate that NMDA receptors are the main type of glutamate receptors involved in the modulation of oligodendrocyte differentiation.

**Characterization of NMDA receptors in differentiating oligodendrocytes.** Next, we studied the expression of NMDA subunits during proliferation and differentiation. Functional NMDA receptors are structurally formed from the NR1 subunit and other subunits. Therefore, we initially assessed the expression of *Grin1*, which encodes NR1, using quantitative RT-PCR at various stages of development in culture. The mRNA transcripts were isolated during neurosphere proliferation, pre-commitment, and after 3 days of differentiation. The level of NR1 transcripts increased dramatically, up to five- to sixfold during the pre-commitment and differentiation stages (Figure 4a). As expected, the level of Olig2 transcripts also increased during differentiation, whereas the expression of the pluripotent gene marker Sox2 remained constant during cell culture (Figure 4a).

The increase in NR1 subunit during differentiation was also confirmed by western blot analysis (Figures 4b and c). NR1 protein was expressed at low levels during proliferation but strongly upregulated (approximately four- to fivefold) during pre-commitment and differentiation. The NR2A subunit was overexpressed during differentiation, whereas the NR2B and NR3 subunits were predominantly expressed during proliferation and pre-commitment, and downregulated later during differentiation (Figures 4b and c).

The functional responses to glutamate were examined using calcium microfluorimetry. Consistent with the pattern of NMDA receptor subunit expression, cells at the pre-committed stage responded to glutamate and DHPG, but not to NMDA (Figure 4d). In contrast, oligodendrocytes in differentiation stages were responsive to both glutamate and NMDA as well as to DHPG (Figure 4d).

Adult neural stem cells express high levels of reactive oxygen species (ROS), which are generated by NADPH oxidase (NOX) and act as second messengers, activating normal cellular processes through the PI3K/AKT pathway.<sup>14,15</sup>

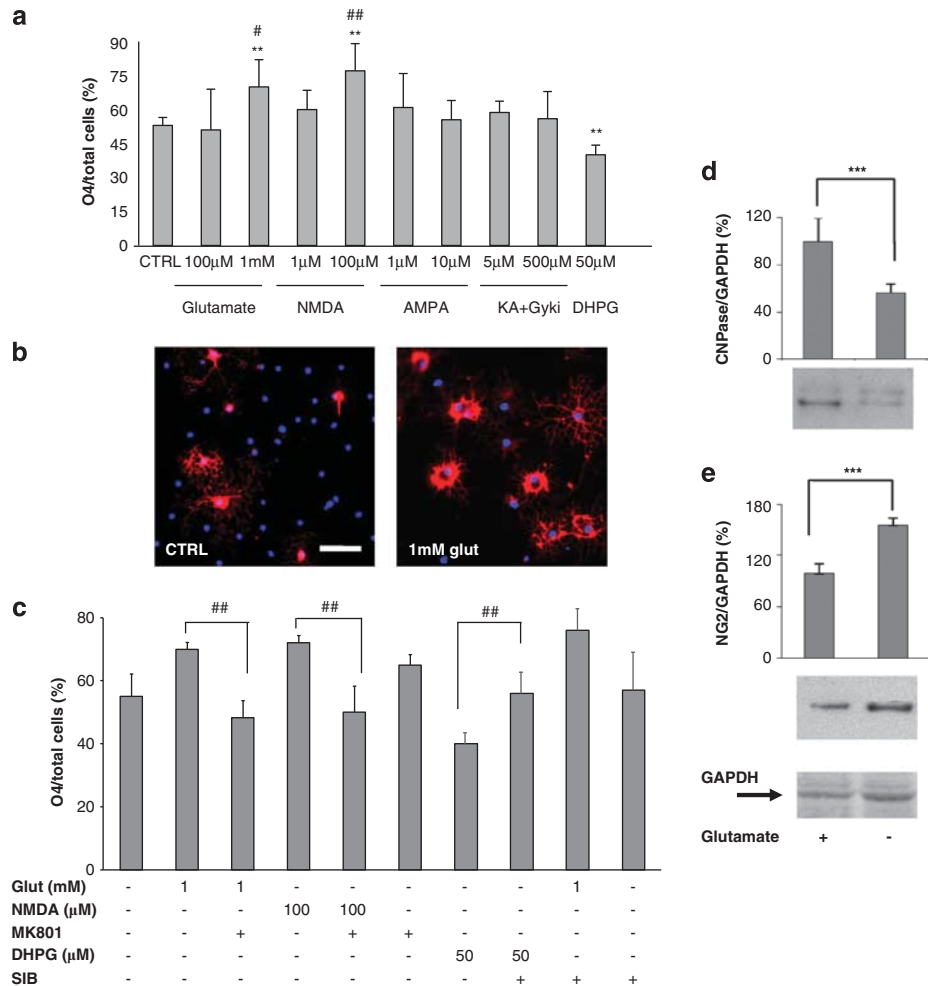


**Figure 2** Effect of glutamate receptor activation on oligodendrocyte differentiation. (a) Neurospheres were differentiated for 3 days in the absence (CTRL) or presence of glutamate or glutamate receptor agonists. Kainate (KA) was used with Gyki53655. The differentiation rate was calculated after immunofluorescence by directly counting the percentage of O4-positive cells compared with the total number of cells counterstained with Hoechst 33258. All experiments with NMDA were performed in the presence of 100  $\mu$ M glycine. Counts represent means  $\pm$  S.E.M. ( $n = 5$  independent experiments, five fields in each).  $**P < 0.01$  versus CTRL,  $^{##}P < 0.01$  versus 1  $\mu$ M NMDA or 100  $\mu$ M glutamate. (b) Representative fields showing O4 staining (red) during differentiation in the absence (CTRL) or presence of glutamate (1 mM). Scale bar = 50  $\mu$ m. (c) The modulation of oligodendrocyte differentiation by glutamate and NMDA was abolished by NMDA receptor antagonist MK801. The differentiation rate was calculated as described above.  $^{##}P < 0.01$  glutamate or NMDA alone versus in conjunction with MK801, and DHPG alone versus in conjunction with SIB 1757. (d and e) Western blots and quantitative histograms with average  $\pm$  S.E.M. showing that glutamate increased the level of CNPase and decreased NG2 protein expression. Protein quantification was performed by densitometric analysis after normalization with GAPDH.  $^{***}P < 0.001$

Because the activation of NMDA receptors can also generate ROS via NOX activation in neurons,<sup>16</sup> we investigated whether this occurs in differentiating oligodendrocytes. ROS levels were higher in differentiating oligodendrocytes when the cells were exposed to glutamate or NMDA, a feature that parallels the proportion of O4 cells in culture (Figures 5a and b). Intracellular ROS levels partially decreased when NOX activity was inhibited by apocynin (Apo) during differentiation (Figure 5a). Notably, we also found that NOX blockade negatively modulated oligodendrocyte differentiation when Apo was present, either alone or in combination with glutamate or NMDA (Figure 5b).

To explore the myelinating potential of differentiated oligodendrocytes, we cocultured pre-committed NG2-positive neurospheres with primary cortical neurons in the presence or absence of glutamate or NMDA. Coculture was

performed with 8 DIV neuronal cultures. This stage was chosen because axonal phosphorylation was maximal,<sup>17</sup> as demonstrated by SMI31 immunostaining (Figure 6a). Before coculture with neurons, pre-committed neurospheres were immune-selected with NG2 antibody (Figures 6b–d). As expected, axons in single neuronal cultures lacked myelin (data not shown), but coculturing pre-committed NG2-positive cells and cortical neurons in differentiating medium yielded myelinated axons (Figures 6e–g). The extent of myelination was evaluated by double immunofluorescence of neurofilament light (NFL) and myelin basic protein (MBP) by counting the number of myelinated axons and assessing myelin elongation (Figure 6h). In control, untreated cultures (Figure 6e), 12% ( $\pm 3$ ) of axons were myelinated and the average myelinated extent of individual axons was 14  $\mu$ m ( $\pm 2$ ). The number of myelinated axons increased up to 20%

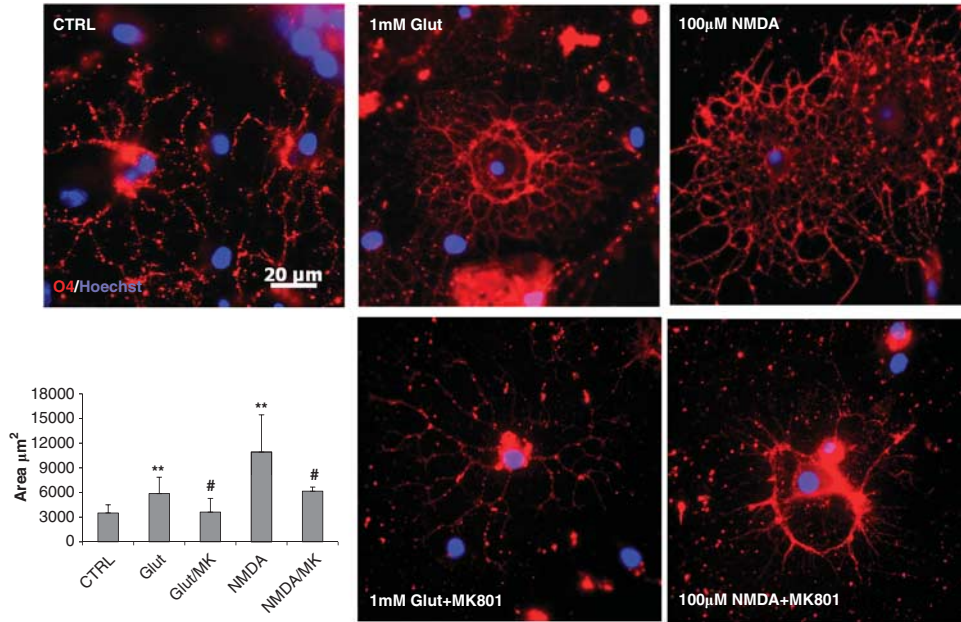


**Figure 3** Glutamate and NMDA induce morphological changes in differentiating oligodendrocytes. Neurosphere cultures were differentiated in the absence (CTRL) or presence of 1 mM glutamate, 100  $\mu$ M NMDA alone, glutamate or NMDA plus 100  $\mu$ M MK801. The area covered by the oligodendrocyte processes was analyzed with a confocal microscope after immunofluorescence for O4 (red). The area was calculated with Axiovision 4.8 (Carl Zeiss, Barcelona, Spain) and expressed in the bar graph as mean  $\mu\text{m}^2 \pm$  S.E.M. of four independent experiments (five fields each). All experiments with NMDA were performed in the presence of 100  $\mu$ M glycine. Blue, Hoechst 33258 staining. \*\* $P < 0.01$  versus control, # $P < 0.05$  versus glutamate or NMDA

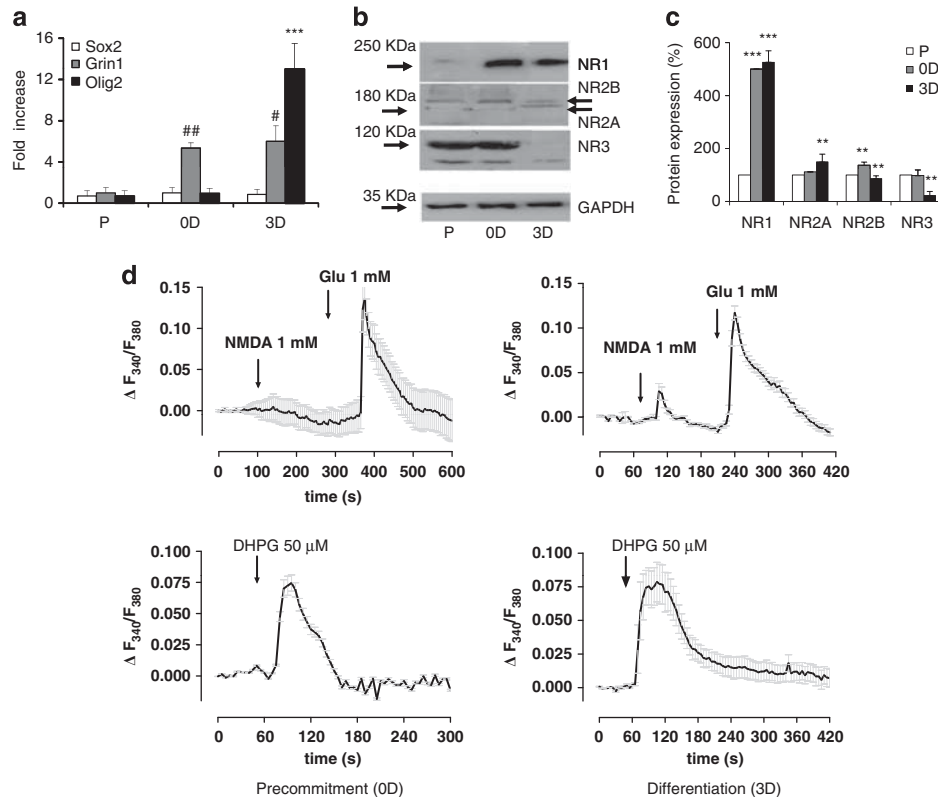


**Figure 4** NMDA receptor expression and function in differentiating oligodendrocytes. (a) Quantitative RT-PCR of NR1 subunit (Grin1), Sox2, and Olig2 transcripts. Quantification was performed after normalization to GAPDH transcripts. # $P < 0.05$ , ## $P < 0.01$ , and \*\*\* $P < 0.001$  versus proliferation (P). (b) Total protein extracts during proliferation (P), after pre-commitment (OD), and after 3 days of differentiation (3D) were subjected to western blot analysis for NR1, NR2A/B, and NR3 protein. (c) The western blot bands were quantified by densitometry after normalization to GAPDH as a percentage of protein expression with respect to proliferation. \*\* $P < 0.01$  or \*\*\* $P < 0.001$  versus proliferation (P). (d) Cytosolic calcium following application of glutamate receptor agonists was measured by microfluorimetry during pre-commitment and 3D. All experiments with NMDA were performed in the presence of 100  $\mu$ M glycine

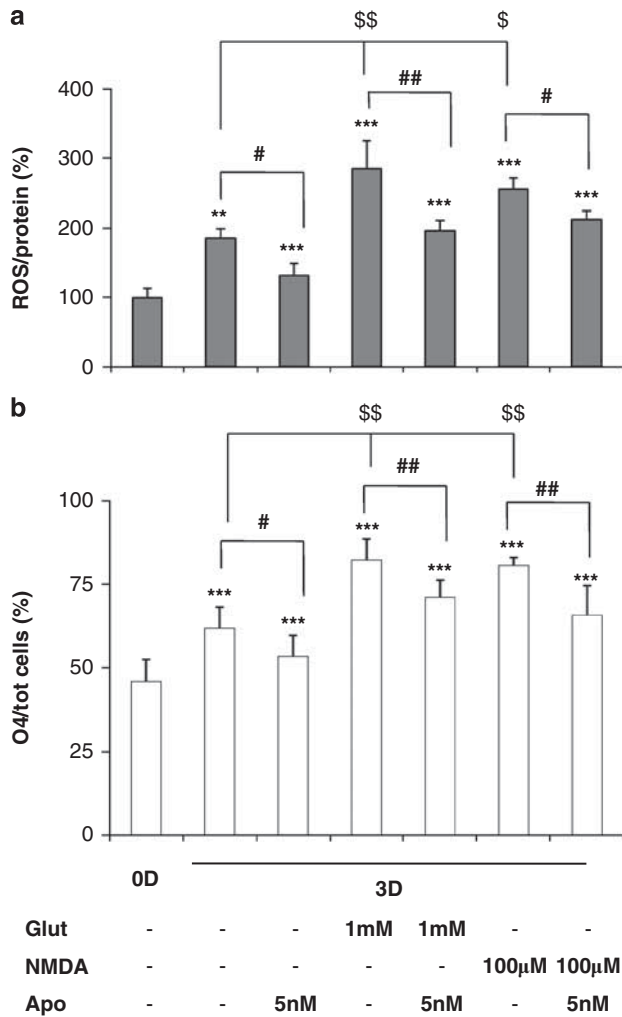


**Figure 5** ROS generation during oligodendrocyte differentiation. (a) ROS were measured after pre-commitment (0D) or after 3 days of differentiation (3D) in the presence of 1 mM glutamate (Glut) or 100 µM NMDA with or without 5 nM Apo. ROS generation was calculated by fluorimetry after normalization to the total protein as a percentage with respect to 0D. (b) NOX-dependent differentiation was calculated as a direct count of O4-positive cells with respect to total cells counterstained with Hoechst 33258. All experiments with NMDA were performed in the presence of 100 µM glycine. The data represent mean  $\pm$  S.E.M. of three independent experiments. \*\* $P < 0.01$ , \*\*\* $P < 0.001$ , # $P < 0.005$ , ## $P < 0.01$ , § $P < 0.05$ , and §§ $P < 0.01$  versus 3D without treatment

( $\pm 7$ ) in cultures treated with 1 mM glutamate (Figure 6f) or 19% ( $\pm 6$ ) with 100 µM NMDA (Figure 6g), whereas axonal stretch covered by myelin was between 19 ( $\pm 2$ ) and 25 µm ( $\pm 5$ ) (Figure 6h).

## Discussion

In the present study, we provide evidence showing that oligodendrocyte differentiation from adult MSCs is modulated by glutamate through the activation of NMDA receptor and the ensuing generation of NOX-dependent oxidative stress.

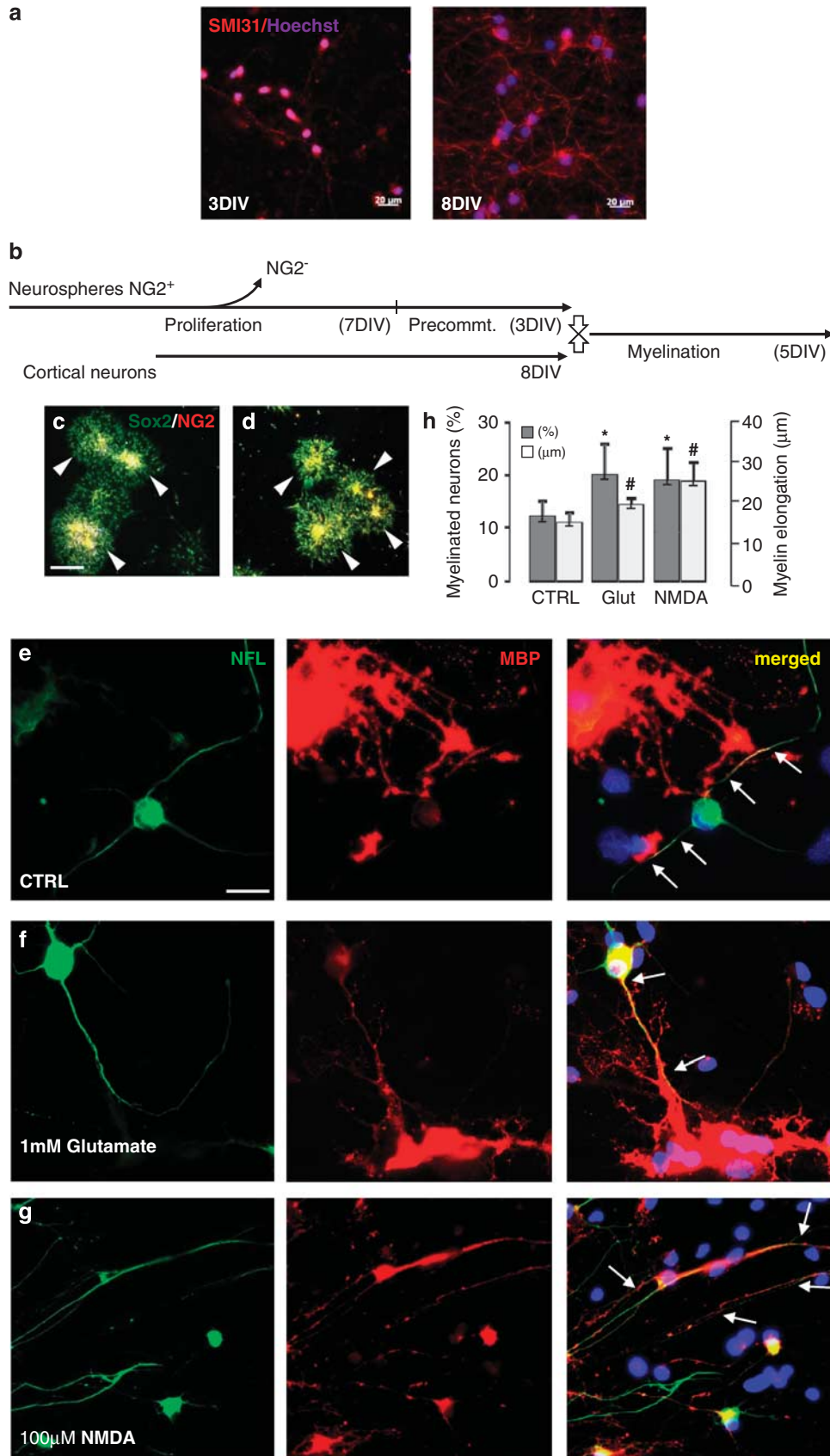
Initially, we developed a protocol to obtain an enriched population of differentiated oligodendrocytes using PEDF to sustain neurosphere proliferation and an intermediate step before differentiation, which was referred to in this study as the

pre-commitment stage. PEDF was chosen because of its expression in the two principal neurogenic niches, the SVZ and subgranular zone.<sup>18–20</sup> Moreover, PEDF is reported to promote the self-renewal of adult neural stem cells *in vitro* through Notch signaling.<sup>19</sup> The proliferation protocol and pre-commitment stage used in the present study allowed us to generate a high number of cells pre-committed to the oligodendrocytic phenotype.

To test the effects of glutamate in oligodendrocyte differentiation, we stimulated rapidly differentiating cells. Under these conditions, we observed that glutamate has a pivotal role in modulating oligodendrocyte differentiation through the activation of NMDA receptors. In contrast, we found that activation of mGluR1/5 reduces oligodendrocyte differentiation. Thus, this suppressive effect may somehow mask the pro-differentiation effects of glutamate on NMDA receptors. NMDA receptor subunits were expressed at all stages of differentiation examined, which is in line with the idea that most cells in the oligodendrocyte lineage have functional NMDA receptors, as shown by electrophysiology in brain tissue slices.<sup>21</sup> In addition, NMDA receptors in differentiating oligodendrocytes are permeable to calcium, though the amplitude of this response was small, which is in agreement with what was reported recently in NG2 cells.<sup>11</sup> The channel maximal open probability ( $P_0$ ) has been reported to span from 0.5 for NR2A-containing receptors to 0.1 for NR2B-containing receptors.<sup>22</sup> However, the role of the NR3 subunit is debated. Together with the structural NR1 subunit, NR3 binds to and is gated by glycine.<sup>23</sup> When expressed as a heterodimer with NR1 alone or with NR2 in *Xenopus oocytes*, NR3 markedly decreases NMDA- and glutamate-induced currents.<sup>24,25</sup> In particular, NR3A subunit, that possesses low affinity for glutamate,<sup>23</sup> can act as a dominant negative element in activating NMDA receptors. When expressed, NR3A subunit binds glycine with a much higher affinity than NR1 subunit, and besides it induces structural modifications by allosteric regulation of NR1.<sup>23</sup> In accordance with these observations, we found that the robust expression of NR3 with weak NR1 subunit expression during proliferation and the pre-commitment stages results in a lack of NMDA receptor function (as a heterodimer with NR1 or as a NR1/NR2/NR3 triheteromer), as suggested by Ulbrich and Isacoff<sup>26</sup>. Thus, our data support the idea that the NR3 subunit is relevant to the modulation of NMDA receptor function during oligodendrocyte differentiation.

Finally, we observed that activation of NMDA receptors in cells of the oligodendrocyte lineage induces NOX-dependent generation of ROS, as observed in neurons.<sup>16</sup> In addition, we found that ROS generated in this manner stimulate oligodendrocyte differentiation as Apo, and inhibitor of NOX prevents this effect. ROS generated after NMDA stimulation activates the PI3K/AKT pathway and it is relevant to NMDA receptor function.<sup>16</sup> Importantly, ROS-mediated enhancements in self-renewal and neurogenesis are dependent on PI3K/Akt signaling<sup>14</sup> and thus, it may also act as a second messenger for sustaining oligodendrocyte differentiation.

In summary, the results of the present study indicate that NMDA receptors are differentially expressed during oligodendrocyte commitment and differentiation from MSCs, and that their activation favors oligodendrocyte differentiation and maturation.



## Materials and Methods

### Cell cultures

**Neurosphere assay.** MSC cultures were prepared from 4- to 7-day-old Sprague-Dawley rat pups. The subventricular zone was isolated and minced with a Mc Illwain tissue chopper (Ted Pella, Inc., Lafayette, IN, USA). SVZ tissue from 2–3 brains was digested for 10 min at 37°C in 5 ml of trypsin/EDTA (Sigma, Madrid, Spain). Digestion was stopped by adding an equal volume of trypsin inhibitor (Sigma) and 0.01% DNase I for 5 min at room temperature. The cell suspension was centrifuged for 10 min at 600 × g and the pellet mechanically dissociated 25 times in NeuroCult medium (Stem Cell Inc., Grenoble, France) using a glass Pasteur pipette and 20 times using 1 ml pipette tips. Undissociated cells were decanted and the single cell suspension counted using the Neubauer method. Cells were seeded in proliferation medium (NeuroCult with 10% neural stem cell factors from Stem Cell Inc., 2 mM glutamine, penicillin/streptomycin mix, 20 ng/ml EGF (Promega, Madrid, Spain), 10 ng/ml bFGF (Promega), 10 ng/ml PEDF (Millipore, Madrid, Spain) at a density of 10<sup>4</sup> cells/cm<sup>2</sup> and cultivated in suspension for 7 days at 37°C, 5% CO<sub>2</sub>. EGF, bFGF, and PEDF were added fresh every 2–3 days.

**Oligodendrocyte differentiation.** After 7 DIV, cells were aggregated as clonogenic neurosphere cultures. Neurospheres were maintained for 3 days in ODM composed of DMEM with 4.5 mg/ml glucose and sodium pyruvate (Gibco, Barcelona, Spain), SATO (100 μg/ml BSA, 100 μg/ml transferrin, 16 μg/ml putrescine, 40 ng/ml thyroxine, 30 ng/ml tri-iodothyronine, 60 ng/ml progesterone, 40 ng/ml selenium, all of from Sigma), 6.3 mg/ml *N*-acetyl-cysteine (Sigma), 0.5 mg/ml insulin (Sigma), 1 μg/ml CNTF (Peprotech, London, UK), and 10 μg/ml NT3 (Peprotech). This step was considered to be the pre-commitment stage before oligodendrocyte differentiation. After 3 DIV, floating neurospheres were attached on cover slips previously treated with polyornithine in the same ODM and differentiated for 1–10 DIV. Differentiation was evaluated by immunofluorescence as a ratio of O4 (from R&D System, Madrid, Spain; used at 1 : 100)-positive cells and total nuclei staining with Hoechst 33258.

**Primary cortical neurons.** Cortical neurons were obtained from the cortical lobes of E18 Sprague-Dawley rat embryos according to previously described procedures.<sup>26–28</sup> Neurons were resuspended in B27 Neurobasal medium (Gibco, Madrid, Spain) plus 10% FBS and then seeded onto poly-L-ornithine-coated glass cover slips (12 mm in diameter) at 10 000 cells/cm<sup>2</sup>. After 24 h, the medium was replaced with serum-free, B27-supplemented Neurobasal medium. The cultures were essentially free of macroglia and microglia, and maintained at 37°C and 5% CO<sub>2</sub>.

**Neurosphere-derived oligodendrocyte and cortical neuron cocultures.** Pre-committed neurospheres were immunoselected for NG2 expression by the immunomagnetic cell isolation system (Easysep, Stem Cell Technology, Grenoble, France). Neurospheres were magnetically labeled and sorted using 1.5 μg of monoclonal NG2 antibody (Abcam, Cambridge, UK). Positive selection was evaluated by double immunostaining with NG2 (Abcam) and Sox2 (Santa Cruz, Biotech., Heidelberg, Germany) antibodies. NG2-positive neurospheres were seeded > 8 DIV primary cortical neurons. The coculture medium consisted of the same proportion of the medium used for cortical neurons and ODM. Cocultures were maintained for 3–5 DIV before confocal analysis with mouse anti-MBP (Millipore, 1 : 1000) and rabbit anti-NFL (Cell Signaling, Barcelona, Spain; 1 : 200). See the scheme in Figure 6b. To prevent toxicity, the cultures were treated with glutamate and NMDA in magnesium-containing medium.

**Immunocytochemistry.** Cell cultures and cocultures were fixed in 4% paraformaldehyde and permeabilized with 0.05% Triton and 5% normal goat serum in phosphate-buffered saline (PBS). Primary antibodies were incubated at different concentrations (O4 (R&D) 1 : 100; NFL (Cell Signaling, Denver, MA, USA) 1 : 300; MBP (Abcam) 1 : 400; SMI31 (Abcam) 1 : 1000; NG2 (Abcam) 1 : 300; and Sox2 (Santa Cruz Biotech) 1 : 100) for 2 h at room temperature and then washed three times with 0.05% Triton in PBS. Secondary conjugated antibodies were incubated for 1 h in the dark at room temperature. All secondary antibodies were diluted at 1 : 200 (Molecular Probes, Barcelona, Spain). After three washes with 0.05% Triton

(except for O4) in PBS, cells or cocultures were stained for 1 min at room temperature with Hoechst 33258 and further washed with PBS. Immunostaining with O4 antibody was performed in PBS without Triton. Finally, cover slips were mounted with Glycergel (Dako, Barcelona, Spain) and analyzed by fluorescence using the Apotome system (Zeiss, Goettingen, Germany).

**mRNA extraction and quantitative RT-PCR.** Neurospheres from a 60-mm petri dish (~ 5000 neurospheres) during proliferation, pre-commitment, and 3 days of differentiation were collected and lysed with Trizol (Invitrogen, Carlsbad, CA, USA). The total RNA extracted was checked on agarose gel and 1 μg was retro-transcribed at 60°C for 60 min using Superscript SSIII (Invitrogen). A 2-μl aliquot of each mRNA were used for real-time quantitative PCR. Commercial primers specific for Grin1, Sox2, and Olig2 were acquired from Qiagen (QuantiTect Primer Assay, Barcelona, Spain), whereas GAPDH primers (forward sequence, 5'-GAAGTCGGTGTCAACGGATT-3'; reverse sequence, 5'-CAATGTCCACTTTG TCACAAGAGAA-3') used for normalization and the standard curve were designed by PrimerExpress software (Applied Biosystems, Madrid, Spain). Real-time quantitative PCR reactions were performed in an ABI PRISM 7000 Sequence Detection System (Applied Biosystems, Carlsbad, CA, USA) as described previously.<sup>29</sup>

**Protein separation and western blot.** Total protein was extracted on ice using RIPA buffer (50 mM Tris-HCl pH 7.4, 1% NP-40, 0.25% Na-deoxycholate, 150 mM NaCl, 1 mM EDTA, 1 mM PMSF, 1 μg/ml each aprotinin, leupeptin, and pepstatin, 1 mM Na<sub>3</sub>VO<sub>4</sub>, and 1 mM NaF) in the presence of protease inhibitor cocktail (Complete, Mini EDTA-free tablets, Roche, San Cugat, Spain). Proteins were denatured for 5 min at 90°C in the presence of sample buffer (6.25 mM Tris pH 6.8, 12.5% glycerol, 2.5% SDS, 0.025% bromophenol blue, and 5% β-mercaptoethanol) and separated by 12% SDS-polyacrylamide gel electrophoresis (10 μg per lane). Separated proteins were transferred overnight at 4°C to a nitrocellulose membrane (Hybond ECL, Amersham Biosciences, Barcelona, Spain) in a wet transference system (Mini Trans-Blot Electrophoretic Transfer Cell, Bio-Rad, Madrid, Spain). Protein transfer was evaluated by Ponceau staining. All membrane incubations were performed in TBST buffer (50 mM Tris Base, 200 mM NaCl, 0.1% Tween-20, pH 7.4). Membranes were saturated in blocking solution (TBST, 5% non-fat dry milk) for 30 min at room temperature with and successively hybridized overnight at 4°C with the different primary antibodies (mAb CNPase, 1 : 500; NG2, 1 : 500; NMDAR1, -R2A/B, or NR3, all 1 : 300; mAb GAPDH, 1 : 500, all from Chemicon, Madrid, Spain). Membranes were washed three times with washing solution (TBST) and incubated for 2 h with different HRP secondary antibodies (all 1 : 5000, Sigma), washed three times, and revealed with peroxidase using ECL (Super Signal West Dura, Pierce, Madrid, Spain). The luminescence of the reaction product was detected by the ChemiDoc XRS Imaging System (Bio-Rad), and the intensity of the bands was quantified using Quantity One (Bio-Rad) software corrected by Gaussian curves.

**Fluorimetric measurement of cytosolic calcium.** Whole neurospheres at different DIV were attached to polyornithine-coated cover slips and loaded with fura-2 AM (5 μM; Invitrogen) in differentiation medium for 45 min at 37°C. Cells were washed in HBSS containing 20 mM HEPES (pH 7.4), 10 mM glucose, and 2 mM CaCl<sub>2</sub> (incubation buffer) for 5 min at room temperature. Experiments were performed in a cover slip chamber continuously perfused with incubation buffer at 1 ml/min. The perfusion chamber was mounted on the stage of a Zeiss (Oberkochen, Germany) inverted epifluorescence microscope (Axiovert 35, Carl Zeiss, Barcelona, Spain) equipped with a 150-W Polychrome IV xenon lamp (T.I.L.L. Photonics, Martinsried, Germany) and a Plan Neofluar 40 × oil immersion objective (Zeiss). Single cells were selected using a high-resolution digital black/white CCD camera (ORCA; Hamamatsu Photonics Iberica, Barcelona, Spain), and image acquisition and data analysis were performed using the AquaCosmos software program (Hamamatsu Photonics Iberica).

**Figure 6** Myelination of cortical neurons by oligodendrocytes derived from SVZ neurospheres. (a) Primary cortical neurons stained with SMI31 at 3 and 8 DIV. Cell nuclei were counterstained with Hoechst 33258. Scale bar = 20 μm. (b) Scheme illustrating the temporal profile of individual and conjunct cultures. Only NG2-positive neurospheres were co-cultivated with primary neurons. Myelination in cocultures was assessed at 5 DIV. (c and d) Neurosphere sorting was assessed by immunofluorescence for NG2 (red) and Sox2 (green) before (c) and after (d) immunoselection. Yellow staining and arrowheads indicate NG2-positive neurospheres. Scale bar = 100 μm. (e and g) Representative fields showing the myelination of axons in control, untreated cultures (e) and cultures treated with 1 mM glutamate (f) or 100 μM NMDA (g). (h) Histogram illustrating the degree of myelination as a percentage of axonal structures (NFL) co-localized with MBP (filled bars) or as myelin elongation expressed in micrometers (empty bars). All experiments with NMDA were performed in the presence of 100 μM glycine. Data represent mean ± S.E.M. of three independent experiments (10–12 fields each).

\**P* < 0.05 versus CTRL, #*P* < 0.05 versus 1 mM glutamate or 100 μM NMDA

**Measurement of intracellular ROS.** Cells were attached to cover slips previously treated with polyornithine and loaded with 30  $\mu$ M CM-H2DCFDA (Invitrogen) for 20 min. ROS levels were normalized with respect to the total protein. Fluorescence was measured using a Synergy-HT fluorimeter (Bio-Tek Instruments Inc., Beverly, MA, USA) using excitation at 485 nm and emission at 527 nm. All experiments ( $n \geq 3$ ) were performed in triplicate and plotted as means  $\pm$  S.E.M.

**Statistical analysis.** Results were evaluated using SPSS software (version 15; New York, NY, USA). All data were tested with the Shapiro-Wilks normality test using the Lilliefors correction and subsequently analyzed by non-parametric tests (Friedman, Kruskal-Wallis, Mann-Whitney *U*, and Wilcoxon tests). Significance was set at  $P < 0.05$ .

### Conflict of Interest

The authors declare no conflict of interest.

**Acknowledgements.** This work was supported by the Spanish Ministry of Science and Innovation (MICINN grants ACI2009-0873 and SAF2010-21547), CIBERNED, Gobierno Vasco, and Universidad del País Vasco.

- Lee J, Gravel M, Zhang R, Thibault P, Braun PE. Process outgrowth in oligodendrocytes is mediated by CNPase a novel microtubule assembly myelin protein. *J Cell Bio* 2005; **170**: 661–673.
- Watkins TA, Emery B, Mulinyawe S, Barres BA. Distinct stages of myelination regulated by  $\gamma$ -secretase and astrocytes in a rapidly myelinating CNS coculture system. *Neuron* 2008; **60**: 555–569.
- Calabresi PA. Considerations in the treatment of relapsing-remitting multiple sclerosis. *Neurology* 2002; **58**: S10–S22.
- Voltz R. Palliative care for multiple sclerosis: a counter-intuitive approach? *Mult Scler* 2010; **16**: 515–517.
- Dutta R, Trapp BD. Mechanisms of neuronal dysfunction and degeneration in multiple sclerosis. *Prog Neurobiol* 2011; **93**: 1–12.
- Lendahl U, Zimmerman LB, McKay RD. CNS stem cells express a new class of intermediate filament protein. *Cell* 1990; **60**: 585–595.
- Yoshihara Y, Kawasaki M, Tamada A, Fujita H, Hayashi H, Kagamiyama H *et al*. OCAM: a new member of the neural cell adhesion molecule family related to zone-to-zone projection of olfactory and vomeronasal axons. *J Neurosci* 1997; **17**: 5830–5842.
- Nishiyama A. Polydendrocytes: NG2 cells with many roles in development and repair of the CNS. *Neuroscientist* 2007; **13**: 62–76.
- Nishiyama A, Komitova M, Suzuki R, Zhu X. Polydendrocytes (NG2 cells): multifunctional cells with lineage plasticity. *Nat Rev Neurosci* 2009; **10**: 9–22.
- Brazel CY, Nuñez JL, Yang Z, Levison SW. Glutamate enhances survival and proliferation of neural progenitors derived from the subventricular zone. *Neuroscience* 2005; **131**: 55–65.
- Hamilton N, Vayro S, Wigley R, Butt AM. Axons and astrocytes release ATP and glutamate to evoke calcium signals in NG2-glia. *Glia* 2010; **58**: 66–79.
- Matute C. Oligodendrocyte NMDA receptors: a novel therapeutic target. *Trends Mol Med* 2006; **12**: 289–292.

- Alberdi E, Sánchez-Gómez MV, Torre I, Domercq M, Pérez-Samartín A, Pérez-Cerdá F *et al*. Activation of kainate receptors sensitizes oligodendrocytes to complement attack. *J Neurosci* 2006; **26**: 3220–3228.
- Le Belle JE, Orozco NM, Paucar AA, Saxe JP, Mottahedeh J, Pyle AD *et al*. Proliferative neural stem cells have high endogenous ROS levels that regulate self-renewal and neurogenesis in a PI3K/Akt-dependant manner. *Cell Stem Cell* 2011; **8**: 59–71.
- Li Z, Dong T, Pröschel C, Noble M. Chemically diverse toxicants converge on Fyn and c-Cbl to disrupt precursor cell function. *PLoS Biol* 2007; **5**: e35.
- Kishida KT, Pao M, Holland SM, Klann E. NADPH oxidase is required for NMDA receptor-dependent activation of ERK in hippocampal area CA1. *J Neurochem* 2005; **94**: 299–306.
- Hsieh ST, Kidd GJ, Crawford TO, Xu Z, Lin WM, Trapp BD *et al*. Regional modulation of neurofilament organization by myelination in normal axons. *J Neurosci* 1994; **14** (11 Part 1): 6392–6401.
- Tombran-Tink J, Barnstable CJ. PEDF: a multifaceted neurotrophic factor. *Nat Rev Neurosci* 2003; **4**: 628–636.
- Ramírez-Castillejo C, Sánchez-Sánchez F, Andreu-Agulló C, Ferrón SR, Aroca-Aguilar JD, Sánchez P *et al*. Pigment epithelium-derived factor is a niche signal for neural stem cell renewal. *Nat Neurosci* 2006; **9**: 331–339.
- Namba T, Yabe T, Gonda Y, Ichikawa N, Sanagi T, Arikawa-hirasawa E *et al*. Pigment epithelium-derived factor up-regulation induced by memantine, an n-methyl-d-aspartate receptor antagonist, is involved in increased proliferation of hippocampal progenitor cells. *Neuroscience* 2010; **167**: 372–383.
- Káradóttir R, Cavellier P, Bergersen LH, Attwell D. NMDA receptors are expressed in oligodendrocytes and activated in ischaemia. *Nature* 2005; **438**: 1162–1166.
- Gielen M, Siegler Retchless B, Mony L, Johnson JW, Paoletti P. Mechanism of differential control of NMDA receptor activity by NR2 subunits. *Nature* 2009; **459**: 703–707.
- Yao Y, Mayer ML. Characterization of a soluble ligand binding domain of the NMDA receptor regulatory subunit NR3A. *J Neurosci* 2006; **26**: 4559–4566.
- Sucher NJ, Akbarian S, Chi CL, Leclerc CL, Awobuluyi M, Deitcher DL *et al*. Developmental and regional expression pattern of a novel NMDA receptor-like subunit (NMDA R-L) in the rodent brain. *J Neurosci* 1995; **15**: 6509–6520.
- Perez-Otano I, Schulte CT, Contractor A, Lipton SA, Trimmer JS, Sucher NJ *et al*. Assembly with the NR1 subunit is required for surface expression of NR3A-containing NMDA receptors. *J Neurosci* 2001; **21**: 1228–1237.
- Ulbrich MH, Isacoff EY. Rules of engagement for NMDA receptor subunits. *Proc Natl Acad Sci USA* 2008; **105**: 14163–14168.
- Cheung NS, Pascoe CJ, Giardina SF, John CA, Beart PM. Micromolar L-glutamate induces extensive apoptosis in an apoptotic-necrotic continuum of insult-dependent, excitotoxic injury in cultured cortical neurones. *Neuropharmacology* 1998; **37**: 1419–1429.
- Larm JA, Cheung NS, Beart PM. (S)-5-fluorowillardiine-mediated neurotoxicity in cultured murine cortical neurones occurs via AMPA and kainate receptors. *Eur J Pharmacol* 1996; **314**: 249–254.
- Vallejo-Illarramendi A, Domercq M, Pérez-Cerdá F, Ravid R, Matute C. Increased expression and function of glutamate transporters in multiple sclerosis. *Neurobiol Dis* 2006; **21**: 154–164.



**Cell Death and Disease** is an open-access journal published by Nature Publishing Group. This work is licensed under the Creative Commons Attribution-NonCommercial-No Derivative Works 3.0 Unported License. To view a copy of this license, visit <http://creativecommons.org/licenses/by-nc-nd/3.0/>